Eur. Phys. J. B **46**, 497–500 (2005)
DOI: 10.1140/epjb/e2005-00279-y

THE EUROPEAN PHYSICAL JOURNAL B

Electrical properties of micrometric metallic dots obtained by porous polymeric membranes

M. Barra[1,a], A. Cassinese[1], F. Chiarella[1], W. Goedel[2,3], D. Marczewski[2], P. Tierno[2], and R. Vaglio[1]

[1] INFM - Coherentia and Università di Napoli Federico II, Dipartimento di Fisica, Napoli, 80125, Italy
[2] University of Ulm, Organic and Macromolecular Chemistry, OCIII, Materials &Catalysis ACII Germany, 89069, Germany
[3] Physical Chemistry, Chemnitz University of Technology, Chemnitz, Germany

Received 19 April 2005 / Received in final form 10 June 2005
Published online 7 September 2005 –

Abstract. We report on the fabrication of micrometric regular metallic arrays obtained by using, as a template, a polymeric membrane with regular pores. The membranes were prepared by embedding hydrophobized silica colloids into a polymer layer and subsequently removing them. We have investigated the electronic transport properties of the metallic arrays as a function of the applied electric field and temperature. Simple current voltage (IV) characteristics present a strong switching behavior with I_{ON}/I_{OFF} ratios up to 10^4. Different temperature dependences of the resistance in the different ranges of the applied electric field have been observed. Finally, the performances of a field effect device (FET), with the conducting channel and insulating layer consisting of a Gold dot array and a STO substrate, respectively, have been investigated. The channel resistivity has been modified at least of two orders of magnitude and a mobility of about 2 $cm^2/V*s$ has been extracted by the analysis of the FET transfer curve.

PACS. 73.23.-b Electronic transport in mesoscopic systems

Introduction

A great deal of research in mesoscopic physics focuses on understanding the physical properties and their size-dependence of granular metals (see [1–3]). Indeed, they represent a unique experimentally accessible tunable system, where both the electronic interaction strength and the degree of disorder can be controlled as well as both metallic and insulating phases of the electrical conductivity can be obtained. In particular, a metal-insulator (MI) reversible transition on dependence of an external control parameter is considered a very attractive feature for the microelectronic applications [4], with an exciting potential for scaling to nanometer dimensions, thus overcoming the predicted silicon technology limits, related to physical phenomena such as short channel effects or tunnelling through a thin gate oxide [4].

However, conventional (and expensive) techniques for nanostructuring these granular systems, such as photo and electron beam lithography, are limited in spatial resolution or writing speed. In this regard, a number of recent investigations have tried to overcome these limitations by using self-organization of block copolymers micelles or particles to generate regular two-and three- dimensional patterns of micrometric and sub-micrometric periodicity [5–8]. Here, we report on the electrical characterization of gold, silver and niobium two dimensional (2D) dot systems obtained by Joule evaporation or sputtering techniques using polymeric porous membranes as a template. Furthermore, in the last section, we have also considered the field effect doping on a gold system obtained through a $SrTiO_3$(STO) film.

Dot array fabrication

The fabrication of the porous membranes was made by hydrophobized silica colloids and nonvolatile liquid trimethylolpropane trimethacrylate (TMPTMA) [8]. The colloids were synthesized by Stöber's method [9] and their surface was hydrophobized by coating them with 3-(trimethoxysilyl) propylmethacrylate (TPM) [10]. Following the procedures of reference [8], a mixture of the colloids, the (TMPTMA) and a volatile solvent (Chloroform/Ethanol mixture) were applied onto the surface of a water-filled Petri dish. After the evaporation of the solvent, a mixed wetting layer with a close hexagonal arrangement of the colloids was formed at the water-air interface. The subsequent photocrosslinking of the liquid and the removal of the colloids made possible for us to obtain polymer membranes with a well defined two-dimensional (2D) arrangement of pores. The size of the pores was precisely controlled by the size of the colloids. The technique in principle allows the realization of arrays with an averaged size ranging between 30 nm and 700 nm [8]. The obtained membranes were easy to be

[a] e-mail: mbarra@na.infn.it

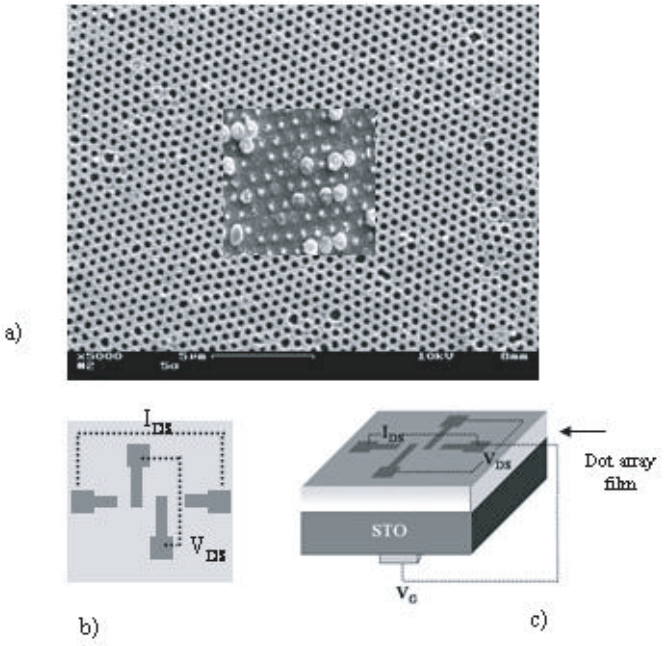

Fig. 1. (a) Scanning electron micrographs (SEM) of a parous membrane. Superimposed is reported, using the same scale, a detail of the granular Gold array obtained. (b) Top view of the four probes arrangement and (c) schematic view of field effect device.

transferred to various substrates and so can be used as masks or moulds, for surface patterning and nanostructure fabrication. In this work, 10×10 mm^2 glass and $SrTiO_3$ (STO) substrates, 0.5 mm thick, were used. As the template for the formation of the granular metallic films, we used porous membranes fabricated by 520 nm silica colloids and with a final diameter of the pore size of 350 nm. The thickness of the membrane was 250 nm. A scanning electron microscope image of such a membrane is shown in Figure 1a. After the deposition of a 300 nm thick metallic layer, the membrane was removed by baking the sample at 450 degree for 20 min.

In case of a gold layer, this results in an array of dots with a well defined averaged dimension, having a mean size in diameter 150 ± 5 nm and a nearest-neighbor distance between them of 400 ± 20 nm. However, in some parts, more complicate structures are also present (inset Fig. 1a). They have a mushroom structure, showing a thinner part of 150 nm and a larger part of roughly 400–500 nm. In this case, the distance between nearest-neighbor mushrooms ranges between 150–50 nm. It should be noted that, by this technique, regular gold arrays have been obtained by sputtering technique when the thickness is less than 25 nm [11]. In our study, in sputtered silver films, we have obtained dot arrays with a size distribution very similar to the gold films. Instead, in sputtered Niobium films, the structure is probably influenced also by the oxidation process (that is always present at the niobium surface) and a more closely-packed structure is realized. In all cases, the dots were clearly disconnected (Fig. 2). However, it should be observed that the surface area investigated for

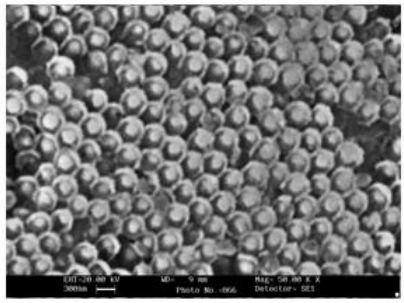

Fig. 2. Scanning electron micrographs (SEM) of a Niobium dot array.

the electronic transport measurements ranges from 25 μm to 125 μm, such that only averaged properties of the grain structure can be tested.

Electrical resistivity characterization

In the fabricated samples, the resistance as a function of temperature and I-V current-voltage characteristics were measured using a standard two-probe technique, where both the voltage application and the current measurement were measured by a Keithley 487 picoammeter. In case of low resistance values, a four probes technique was used, where a constant current I_{DS} was injected between the currentpads and the drain-source voltage drop V_{DS} is recorded (Fig. 1b). Electrical contacts (200 μm wide) are grown using suitable stencil-steel masks. In the field effect devices (Fig. 1c), the gate is deposited on the back side of a 0.5 mm thick $SrTiO_3$(STO) substrate.

In Figure 3, a typical I-V curve for the silver system obtained with a channel length of 125 μm is reported. As shown, around 11 V, corresponding to an electrical field of about 10^3 V/cm, the current increases more than four orders of magnitude within a range of 1 V. Below the breakdown voltage, the resistance is close to 1 GΩ, and above the breakdown value the resistance is about 10 KΩ remaining almost constant up to 20 V. The estimated resistivity values ρ are about $5 \times 10^4\,\Omega$m and 0.5 Ωm, respectively.

The resistance values for voltages below and above the breakdown fields are reproducible and almost the same for all samples fabricated under the same conditions. Instead, the value of the breakdown field is sample dependent and is reproducible between different runs on the same sample at a level of $\pm 10\%$. However, hysteretic behavior, typical for discontinuous conducting structures [12], were observed. A detailed analysis of this effect is beyond the scope of this work and will be reported elsewhere. According to our experimental measurements, the current regimes above and below the breakdown threshold could involve different conduction mechanisms. To further investigate this question, measurements of the channel resistance as function of the temperature have been carried out for different applied voltages. For instance, the inset of Figure 3 reports the resistance dependence on temperature obtained when a 50 V voltage is applied and

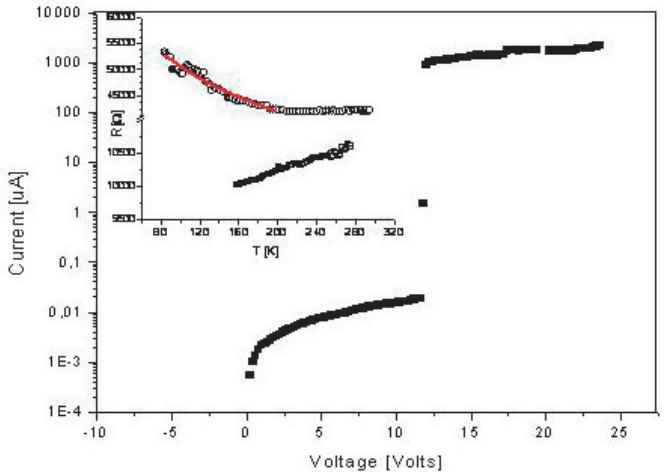

Fig. 3. I-V characteristic observed on Silver system. In the inset, temperature dependence of the resistance measured, with an applied voltage of 11.5 V (circles), and 50 Volts (squares) are shown. The continuous curve represents a fit obtained with $R = R_0(1 - \alpha \ln T)$ relation.

a "metal-like" behavior ($dR/dT < 0$) is observed. However, it should be noted that a decrease of only 5% of the resistance in a range of 100 K (275 K $< T <$ 175 K) was observed, which cannot be ascribed to a simple direct conduction mechanism. Measurements performed just below the breakdown value, corresponding to a resistance value about 40 KΩ, present a slight decrease of the resistance (less than 1%) by decreasing the temperature, followed by an increase of the resistance at low temperatures ($T <$ 220 K). In this temperature region, the data are well fitted by the logarithmic power law (continuous curve): $R = R_0(1 - \alpha \ln T)$ with $\alpha = 0, 115$. It is useful to observe that the logarithmic power dependence and this value of α are typical for 2D structures [1]. At lower voltages, a well-recognized insulating behavior is observed, starting from $R = 1$ GΩ at room temperature and increasing up to $R = 100$ GΩ at 180 K, limited by the experimental set-up.

Similar measurements have been obtained as well on gold samples even if the breakdown in the I-V curves is less pronounced. In this case the channel length is 25 μm and the resistance measured ranges between 10 KΩ and 1000 KΩ, corresponding to an average resistivity of about 2 Ωm and 2×10^2 Ωm, respectively. The crossover between the two regimes takes place at around 250 KΩ, for a voltage of few Volts (1–2 Volts) and is smoother than in the silver samples. By our analysis, the gold system seems to have a more metallic character than the silver system and the resistivity versus temperature dependence in the metallic region from $T = 295$ K to 220 K shows a decrease of about 20%, as shown in Figure 4. This can likely be related to a better quality of the sample which is not affected by the oxidation process. In Figure 4, insulating behavior, obtained during the same measurements by opportunely switching the applied voltage at about $T = 220$ K, is also presented. Finally, concerning the niobium samples, no

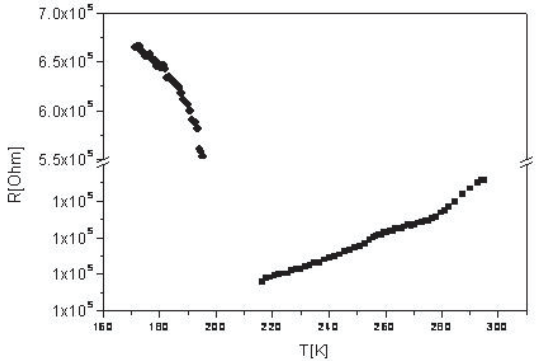

Fig. 4. Temperature dependence of a gold sample resistance (a) above and (b) below the breakdown.

switching phenomenon in IV curves was observed for applied voltage up to 500 V and, for all the investigated samples, the resistance temperature dependence showed a clear insulating behavior, similar to that found for gold and silver samples at low voltages. In our opinion, this behavior can be also ascribed to an oxidized niobium layer always present at the grain boundaries on the film surface [13].

Field effect measurements

As far as the field effect device (FET) is concerned, a prototype device was fabricated according to the classical structure of the thin film transistors (TFT) [14]. In our study, the gold dot array represents the conducting channel, while the insulating layer is realized by a STO substrate. Unlike the conventional metal-oxide semiconductor field effect devices (MOSFETs) based on doped crystalline silicon, thin film transistors operate in the accumulation-depletion regime and not in inversion regime. The source and drain gold contacts have been evaporated according to the geometry in Figure 1b, which makes possible either the four or two probe techniques. The same concept was recently adopted in the field-effect tuning of carrier density in $Nd_{1.2}Ba_{1.8}Cu_3O_y$ thin films [15]. STO substrates are particularly suitable for gate oxide, because of its high dielectric constant ε_r. In our work, experimental measurements of ε_r have been carried out and a value of about 300 at room temperature, in very good agreement with data present in literature [16], has been found. It is worth to mention that this ε_r value guarantees a measured insulator capacitance C_i per unit area of about 0.5 nF/cm^2, when a thickness of 500 μm is considered. Consequently, the induced charge density per volt can be estimated to about $\frac{\Delta n_S}{V_{\text{gate}}} = 3.31 \times 10^9 \frac{1}{\text{cm}^2 \times \text{Volt}}$. According to the basic FET working principle, the electrostatic doping by the gate voltage changes the number of carriers, thus modulating the channel resistance, which however, in our case, is strongly dependent also on the applied V_{DS}. In this regard, Figure 5 reports the channel resistance of the gold granular channel obtained with four subsequently increasing voltages ($V_{\text{DS1}} < V_{\text{DS2}} < V_{\text{DS3}} < V_{\text{DS4}}$).

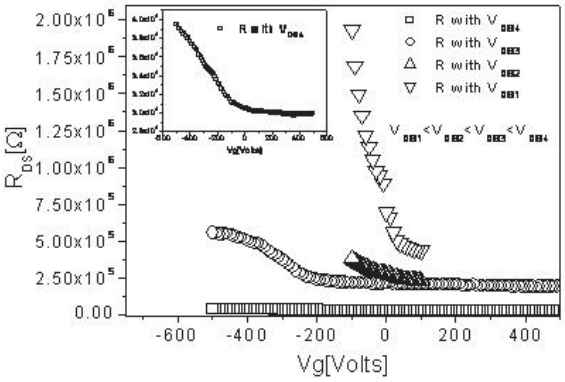

Fig. 5. Resistance as a function of a gate voltage observed on a Gold granular system for different channel voltages $V_{\rm DS1}$ (Down triangles) < $V_{\rm DS2}$ (Up triangles) < $V_{\rm DS3}$ (Circles) < $V_{\rm DS4}$ (Squares). In the inset, magnification for $V_{\rm DS4}$ curve.

The field effect modulation provides an increase of the channel resistance R_{DS} for negative gate voltages, which is consistent with fact that the carriers are electrons. Moreover, the modulation effect is higher for increasing $R_{\rm DS}$ (decreasing $V_{\rm DS}$). It is possible to observe that in the $\frac{dR}{dT} > 0$ (metal-like) regime (squares, $R_{\rm DS} = 20$ KΩ), the field effect modulation (<1%) is negligible in case of positive gate voltages, while a small modulation of the resistance (≈20%) is present for very large negative applied gate voltages ($\mathrm{V_{gate}} < -300$ Volts) as a consequence of the depletion effect (see the inset in Fig. 5). On the contrary, in the case of V_{DS1} (down triangles, $\frac{dR}{dT} < 0$),the modulation effects are much more evident. Consequently, the 600 KΩ resistance at $V_{\rm gate} = 0$ V is changed up to about 1.8 MΩ for $V_{\rm gate} = -100$ V (depletion effect), reaching a minimum value of 400 KΩ at $V_{\rm gate} = -100$ V (accumulation effect). In this region, by the analysis of the linear transfer characteristic ($I_{\rm DS} - V_{\rm GS}$) and the related transconductance $g_m = \left|\frac{\partial I_{ds}}{\partial V_{\rm Gate}}\right| = \frac{W \times C_i \times \mu_e}{L \times V_{\rm DS}}$, with W and L the width and the length of the FET channel, respectively, we estimated the equivalent mobility μ_e to about 2 $\mathrm{cm^2/V^*s}$. It is worth mentioning that this value allows the fabrication of thin film transistors for different practical applications (i.e. active matrix displays) and is better than those of other metal-insulator field effect devices, recently reported and based on perovskite oxides [17]. Finally, it is interesting to note that the intermediate values of $V_{\rm DS}$ (up triangles and circles) produce an intermediate range of the modulation.

Conclusions

In conclusion, we report on the realization and electrical characterization of micrometric silver gold and niobium granular systems obtained by using regular porous membranes as a template and without the use of a lithography process. The samples can be induced in a reversible way to display different temperature dependences of the resistance by applying different $V_{\rm DS}$ values, as demonstrated by the resistivity measurements as a function of the temperature. Using a field effect device (FET), we modified the number of carriers of a gold system and a modulation of the resistivity at least of two orders of magnitude was observed, as a result of both accumulation and depletion effects. Unlike the traditional FET, the electrostatic doping effects are strongly dependent also on the applied $V_{\rm DS}$, such that the tunability range of the electron transport properties is largely broadened. This feature appears as a promising step to realize devices of interest both for fundamental studies and practical applications. Future work will be devoted to optimize the fabrication process and to investigate the possibility to scale the device size on smaller scales.

The authors thank the support of M. Möller, K. Landfester, B. Rieger (University of Ulm), H. Auweter and R. Iden (BASF). The technical support of A. Maggio and S. Marrazzo is gratefully acknowledged. Finally we thank also Prof. Dr Paul P. Walter (University of Ulm) for the use of the Scanning Electron Microscope.

References

1. A. Gerber, A. Milner, G. Deutscher, M. Karpovsky, A. Gladkikh, Phys. Rev. Lett. **78**, 4277 (1997)
2. R.W. Simon, B.J. Dalrymple, D. Van Vechten, W.W. Fuller, S.A. Wolf, Phys. Rev. B **36**, 1962 (1987)
3. I.S. Beloborodov, K.B. Efetov, A.V. Lopatin, V.M. Vinokur1, Phys. Rev. Lett. **91**, 246801 (2003)
4. D.M. News, J.A. Misewich, C.C. Tseui, A. Gupta, B.A. Scott, A. Schrott, Mott tansition field effect transistor, Appl. Phys. Lett. **73**, 780 (1998)
5. T. Hashimoto, K. Tsutsumi, Y. Funaki, Langmuir **13**, 6869 (1997)
6. M. Templin, A. Franck, A. Du Chesen, H. Leist, Y. Zhang, R. Ulrich, V. Schaedler, U. Wiesner, Science **278**, 1795 (1997)
7. M. Haupt, S. Miller, A. Ladenburger, R. Sauer, K. Thonke, J. Spatz, S. Riethmueller, M. Moeller, F. Banhart, J. Appl. Phys. **91**, 6057 (2002)
8. Hui Xu, Werner A. Goedel, Langmuir **18**, 2363, (2002); Feng Yan, Werner A. Goedel, Chemistry of Materials **16**, pp 1622–1626 (2004); Feng Yan, W.A. Goedel, Advanced Materials **16**, 911 (2004)
9. W. Stober, A. Fink, E. Bohn, J. Colloid Interface Sci. **26**, 62 (1968)
10. P. Philipse, A. Vrij, J. Colloid Interface Sci. **128**, 121 (1998)
11. A. Ladenburger, R. sauer, K. Thonke, F. Yan, W.A. Goedel, in preparation
12. A. Heimann, *Polymer Films with embedded metal Nanoparticles* (Springer, 2003)
13. J. Hallbritter, J. Appl. Phys. **97**, 083904 (2005)
14. G. Horowitz, Organic Field Effect Transistors, Advanced Materials **10**, 365, 1998
15. A. Cassinese, G.M. DeLuca, A. Prigiobbo, M. Salluzzo, R. Vaglio, Appl. Phys. Lett. **84**, 3933 (2004)
16. D. Matthey, S. Gariglio, J.-M. Triscone, Appl. Phys. Lett. **83**, 3758 (2003)
17. K. Ueno, I.H. Inoue, T. Yamada, H. Akoh, Y. Tokura, H. Takagi, Field effect transistor based on $KTaO_3$ peroskite, Appl. Phys. Lett. **84**, 3726 (2004)